Efficient removal of ultrafine particles from diesel exhaust by selected tree species: implications for roadside planting for improving the quality of urban air

Huixia Wang [1, 2], Barbara A Maher[2], Imad AM Ahmed[3] & Brian Davison[2]*

[1] School of Environmental and Municipal Engineering, Xi'an University of Architecture & Technology, Xi'an, 710055, Shaanxi Province, PRC

[2] Lancaster Environment Centre, University of Lancaster, Lancaster, LA1 4YQ, U.K.

[3] Department of Earth Sciences, University of Oxford, Oxford, OX1 3AN, U.K.

*Corresponding author: b.maher@lancaster.ac.uk

KEYWORDS: particulate matter (PM); human health; nanoparticles; deposition velocity; particle removal by leaf capture; magnetic particles; transition metals

ABSTRACT

Human exposure to airborne ultrafine (<<1 μm) particulate pollution may pose substantial hazard to human health, particularly in urban roadside environments where very large numbers of people are frequently exposed to vehicle-derived ultrafine particles (UFPs). For mitigation purposes, it is timely and important to quantify the deposition of traffic-derived UFPs onto leaves of selected plant species, with particularly efficient particle capture (high deposition velocity), and which can be installed kerbside, proximal to the emitting vehicular sources. Here, we quantify the size-resolved capture efficiency of UFPs from a diesel vehicle exhaust by nine temperate-zone plant species, in wind tunnel experiments. The results show that silver birch (79% UFP removal), yew (71%) and elder (70.5%) have very high capability for capture of airborne UFPs. Metal concentrations and metal enrichment ratios in leaf leachates were also highest for the post-exposure silver birch leaves; scanning electron microscopy shows UFPs concentrated along the hairs of these leaves. For all but two species, magnetic measurements demonstrate substantial increases in the concentration of magnetic particles deposited on the leaves after exposure to the exhaust particulates. Together, these new data show that leaf-deposition of UFPs is chiefly responsible for the substantial reductions in particle numbers measured downwind of the vegetation. It is critical to recognise that the deposition velocity of airborne particulate matter (PM) to leaves is species-specific; and often substantially higher (~10 to 50 times higher) than the 'standard' V_d values (e.g. 0.1 – 0.64 cm s^{-1} for $PM_{2.5}$) used in most modelling studies. The use of such low V_d values in models results in major under-estimation of PM removal by roadside vegetation, and thus misrepresents the efficacy of

selected vegetation species for substantial (>> 20%) removal of PM. Given the potential hazard to health posed by UFPs, and the removal efficiencies shown here (and by previous roadside measurements), roadside planting at PM 'hotspots' of selected species (maintained at or below head height) can contribute substantially and quickly to improvement in urban air quality, and reductions in human exposure. These findings can contribute to development and implementation of mitigation policies of traffic-derived PM on an international scale.

Introduction

1.1 Airborne particulate matter, and ultrafine particles

Airborne particulate matter (PM) is a health hazard on a global scale. Ultrafine particles (UFPs, aerodynamic diameter < 1000 nm), with a lifetime in the atmosphere ranging from a few seconds to several days, may pose particular risk to the health of the very large populations living, commuting and working in polluted urban environments, especially near major roadways[1]. UFPs have been shown to penetrate the respiratory system, enter the blood circulation, transfer to extra-pulmonary organs[2-3], and may also enter the brain directly via the olfactory bulb[4-5]. UFPs may be more toxic than microscale particles with the same chemical composition and at the same mass concentration owing to their very large surface area, increased chemical reactivity and ease of cell penetration[6-9].

Airborne UFPs can be derived both from anthropogenic and natural sources (e.g. biomass burning), but in many urban centres, motor vehicles are the primary emission sources of UFPs to the atmosphere, particularly in the morning and afternoon/evening rush hours[10-12]. Primary, vehicle-derived UFPs are produced directly from fuel combustion[13-14], engine wear[15] and from frictional processes, especially brake wear[16-17]. Re-suspension of road dust provides multiple opportunities for post-emission supply of airborne UFPs[18]. Primary, vehicle-derived UFPs are often enriched in highly bioreactive transition metal species, especially Fe (both Fe^{2+} and Fe^{3+}), Cu, Mn and Cr[12, 19], and other metals including Zn, Ni, V, and Pb[12, 20]. Secondary UFPs form in the atmosphere through photochemical reactions involving gaseous precursors and post-emission nucleation and condensation processes[10, 21].

Currently, policies for regulation of airborne PM are based on mass concentrations, of PM_{10} and/or $PM_{2.5}$ (of aerodynamic diameter <10 μm or < 2.5 μm, respectively). The contribution of UFPs to such mass-based metrics is minimal (< 10%), whereas they make up ~80% or more of the PM number[14, 21-22].

Most of the PM emitted from vehicle exhausts lies within the $PM_{1.0}$ size range, with median mass diameter between ~100 and 200 nm and a median number diameter of ~20 nm[23-24]. Emissions control strategies, based on engine design and after-treatment devices, have reduced the average mass of particle emissions, but had limited success in reducing UFP numbers. Indeed, some studies have reported increased UFP numbers[25] and increased UFP toxicity[26-27] with the introduction of after-treatment devices. Hence, it is timely and important to identify feasible and efficient technologies that can capture airborne UFPs, thus reducing human exposure and damage to health.

1.2 The effects of roadside vegetation on airborne PM: modelling and measurements.

Roadside vegetation has the potential to decrease airborne PM concentrations, through PM deposition on leaves, but also to increase PM concentrations, by impeding airflow and reducing the dispersion of PM. As noted by recent reports[28], and reviews[29], many modelling-based studies (using computational fluid dynamics, CFD, to simulate PM emission, dispersion and deposition) have indicated rather small reductions, i.e. a few percent, in PM_{10} or $PM_{2.5}$ concentrations by deposition onto roadside vegetation[30-33]. If robust, such model-derived outcomes indicate that roadside planting schemes are unlikely to produce any large reductions ('> 20%') in PM_{10} or $PM_{2.5}$ concentrations. Indeed, AQEG[28] warns against 'campaigning zeal' in 'popular publications' in communicating the likely improvements in air quality achievable with roadside vegetation.

In a recent review[34] of some measurement-based (roadside, and wind tunnel) studies, the reported removal efficiencies of PM concentrations by roadside vegetation vary enormously, from enhancement of $PM_{2.5}$ (by up to 95%) to reductions (in, variably, PM, total suspended particulates, UFPs, PM_1, $PM_{2.5}$, PM_{10}) of ~2 to 90%.

A fundamental factor appears to be key to both the parsimony of the model estimates and diversity of the measured PM removal rates. That factor is the (mis)treatment of particle deposition velocity (V_d) to leaf surfaces. Notwithstanding that particle deposition rates depend on a range of factors, including particle diameter, PM concentration and wind speed, the critical influence of *species-specific* leaf surface properties on controlling particle deposition rates, capture, and agglomeration appears to have been under-recognised in measurement-based studies, and substantially under-parameterised (i.e. typically by 5 to 50 times), in the majority of CFD models[12, 35].

Leaf number, size, surface structures and the thickness, structure and composition of epicuticular wax play critical roles in determining V_d and particle retention[36-40]. For example, using magnetic particle loadings as a proxy for PM_{10}, Mitchell et al.[39] reported (magnetic) V_d values varying for different plant species as a function of leaf micro-topography, especially hairiness and rugosity. Lowest V_d values ranged from 0.5 to 0.9 cm s^{-1} for sweet chestnut, elder, elm and willow; intermediate values from 1.3 to 1.9 cm s^{-1} for sycamore, horse chestnut, ash and maple; higher V_d values, from 2.4 to 4.6 cm s^{-1}, for lime, beech and silver birch. Deposition velocities of 10 cm s^{-1} have been reported for grassland[41] and Douglas fir for PM_{10}[42] while Freer-Smith et al.[43] have reported V_d values exceeding 30 cm s^{-1} for maple, pine and cypress for $PM_{1.0}$.

In contrast, and critically, many modelling-based studies choose to use 'standard' deposition velocity values as low as 0.64 cm s^{-1} or 0.1 cm s^{-1} for $PM_{2.5}$ [30, 44-45], or 0.2 cm s^{-1} for PM_{10} [33]. Such values seem both low and indiscriminate, despite available data showing the species-specific nature of this key term. It is therefore unsurprising (and indeed self-fulfilling) that such modelling studies typically identify dominance of the aerodynamic (reduced ventilation) over the depositional effects of roadside vegetation.

Based on the *measured* deposition velocities, then installation, close to the emitting vehicle sources, of selected species with optimal V_d values, and controlled height and permeability, can substantially reduce concentrations of traffic-derived PM (Fig. S1), whether at the roadside[46] or in adjacent indoor environments.

For example, for a V_d of 4.6 cm s^{-1} (e.g. silver birch), and leaf surface area of 125 m^2/tree (canopy diameter 8m), 8 trees/100 m street length would remove 50% of the traffic-derived PM_{10} (Fig. S1). Such removal rates tally with published studies. In a street canyon setting, leaf capture of PM by young, roadside silver birch trees was associated with major reductions (60 – 80%) in adjacent indoor concentrations of $PM_{1.0}$, $PM_{2.5}$ and PM_{10}[12].

The orientation of roads in relation to predominant wind directions must also, of course, be taken into account, to ensure effective design of any newly-installed vegetation whether at the roadside, or within the roadway (e.g. as central lines, or lane separators).

Not only species selection but management is important since tall trees (> rooftop height) and high canopy density[47] can increase airborne PM mass concentrations, especially in street canyons, by obstructing airflow and reducing PM dispersion, effectively trapping the pollutants[33]. Additionally, some plant species can act as sources of biogenic volatile organic compounds (VOCs) to the urban atmosphere. For example, oxidation of isoprene, monotrepenes and sesquiterpenes can enhance secondary formation of $PM_{2.5}$ and of ground level ozone[48-50]. Albeit less hazardous than UFPs, the pollen of some species can trigger allergic rhinitis (hay fever).

For humid areas like Lancaster, the PM capture capability of birch leaves is renewed through PM wash-off by abundant rainfall[39, 51]. In drier areas, watering schemes might enable optimized PM removal by vegetation. The potential for contamination of the roadside soil[52] might require management, depending on the number of years of planned exposure time.

Depending on climate (especially humidity, rainfall), some species are likely to offer permanent take-up of PM via particle entry through the leaf stomata, especially in the case of waxy, evergreen leaves. Hence, combining tested, efficient, deciduous and evergreen species might optimize PM removal through the entire year.

In terms of management, the selected roadside vegetation barrier, comprising selected, high-deposition-velocity, PM-tolerant mixed evergreen and deciduous species, should be kept well below roof height[35], and pruned to prevent development of a dense canopy crown, in order to facilitate atmospheric dispersion of PM. Selected species of trees, managed as hedges ('tredges'©), may thus provide the best option for immediate improvement of air quality, especially in PM 'hotspots', wherever the most, and the most vulnerable people (e.g. young children) receive the greatest PM exposure.

1.3 Vegetation impacts on UFPs

Despite their abundance in the urban atmosphere and their potential toxicity, UFP removal by plants has so far received relatively little attention. Field measurements to quantify the influence of urban plants on UFPs and particle number concentrations (PNCs) are few. In Raleigh, Carolina, Baldauf et al.[53] found PNCs reductions of 15 – 50% at distances up to 10s of metres behind a (discontinuous) noise barrier; combined noise and vegetation barriers consistently reduced the PNCs more efficiently than noise barriers alone.

For a major road in Guildford, UK, Al-Dabbous and Kumar[54] reported ~37% reduction in PNCs by a coniferous vegetation barrier, during intervals with cross-road wind directions. Lin et al.[55] reported 38 to 64% reduction in UFPs (14 to 102 nm) concentrations behind a deciduous roadside vegetation barrier when in leaf, but no reduction in winter without foliage.

Fewer studies have examined the effects of different types of vegetation on reducing UFP numbers. Using pine and juniper branches in a wind tunnel, Lin and Khlystov[56] found UFP removal efficiency to be directly proportional to the vegetation packing density, and inversely proportional to particle size and wind speed. Freer-Smith et al.[43] found that V_d values were dependent on plant species, particle size and ambient PM concentrations. For some coniferous species, they reported V_d values for UFPs as high as 25 to 36 cm s^{-1} at a busy road, and 12 to 30 cm s^{-1} at a parkland site. Hwang et al.[57] studied five different vegetation types in a deposition chamber. They reported higher V_d for UFPs for needle leaf compared with broadleaf trees; the leaf surface roughness also influenced the deposition efficiency.

In summary, a limited number of studies has examined the removal efficiency of traffic-produced UFPs by different plant species. Given limited space in urban areas, it is important that the most effective plant species for UFP removal should be selected for urban greening. Here, we examine, in a wind tunnel, the size-resolved removal of UFPs by nine plant species: silver birch (*Betula pendula*), yew (*Taxus baccata*), nettle (*Urtica fissa*), beech (*Fagus sylvatica*), cherry (*Prunus avium*), elder (*Sambucus nigra*), maple (*Acer campestre*), hawthorn (*Crataegus monogyna*) and ash (*Fraxinus excelsior*). Our new data indicate that selected plant species can remove by surface deposition substantial amounts (> 50%) of ultrafine exhaust-derived PM, and of the heavy metals contained within the high particle number concentrations of this PM fraction. Fast, non-destructive magnetic measurements provide an effective indicator of leaf particle deposition. Scanning electron microscopy can identify the major leaf micro-sites associated with greatest particle accumulation. Hence, roadside planting of carefully-selected and managed plant species can effectively mitigate exposure of road users and adjacent residents (especially vulnerable groups like school children) to UFP pollution near major roads. Careful testing and selection of the most efficient species can readily improve air quality.

2. Experimental methods

2.1 Plant Species

UFP removal efficiency was measured in a rectangular wind tunnel (200 cm long, 75 cm wide, 75 cm high, Fig. S2). Nine plant species with different leaf surface characteristics and particle deposition velocities were selected based on our previous study[39], including silver birch, yew, nettle, beech, cherry, elder, maple, hawthorn and ash. These species are widespread in temperate regions, have different leaf retention behavior (i.e., deciduous vs evergreen species) and different leaf morphologies (i.e., broad leaves vs needles) and micro-topographies, which are expected to have an influence on UFP deposition and accumulation (Table S1, Supporting Information).

To obtain 'clean' leaves, plant species were collected after rainfall from Lancaster University campus (maple, ash, hawthorn, beech, cherry, elder) and Williamson Park, Lancaster (yew, silver birch, nettle), as far as possible from roads. Branches (~60 cm in length) of each species, freshly cut on the day of the measurements, were supported vertically and uniformly as a vegetation block (i.e. with very similar leaf area index, LAI, values, Table S1) to ensure that most of the air stream passes through them (Fig. S2, Supporting Information). Particles were emitted from the exhaust of an idling diesel engine (2.1 litre, with catalytic converter; BS EN590 Standard diesel fuel), and injected via smooth plastic tubing into the wind tunnel. A fan positioned at the centre of the front sidewall was used to produce steady airflow, of 1.0 m s^{-1} (typical for the Lancaster area in summer[58], and to mix the exhaust stream with the airflow.

2.2 Particle number concentrations and size distributions

A GRIMM model 5.400 scanning mobility particle sizer (SMPS), comprising a long differential mobility analyser (DMA, model 5.5-900), was used to measure particles in 44 size categories, between 9.8 and 874.8 nm, to obtain the size distribution and count PNCs over consecutive 7 min intervals. Particle sampling was carried out via plastic tubing (~60 cm) connected first to a sampling port located upwind (~20 cm) and then downwind (~20 cm) of the vegetation, to sample continuous PNCs and particle size distributions. PNCs and size distribution measurements were first made in the absence of any vegetation for four separate 7 min. intervals. Measurements were then made first, upwind and then, downwind of the different vegetation species, over successive sampling durations; 5 × 7 mins for each plant species. For each of the plant species, the collection efficiency was measured at a wind speed of 1.0 m s^{-1}, typical in summer in the study area (Lancaster, U.K.).

At the end of the experiment, ~5% of the total leaves from each vegetation block was weighed (Oertling KC22 microbalance) then scanned, and leaf area measured through counting image pixels. Total foliage area was determined by the mass proportion of the scanned leaf weight to total weight and leaf area; the total leaf area was divided by the crown area to determine the LAI, to ensure comparability between the species removal efficiencies (the LAI values varied very little, from 7.2 to 8.8, Table S1).

Leaf samples of each species were collected before exposure to the diesel exhaust (here labelled as 0 minutes) and then after successive exposure intervals (i.e. after 2, 5, 10, 20, 30, and 35 minutes), using gloves to avoid contamination. The leaves were stored (upper surface to upper surface) in ziplock bags, at 4 °C, prior to scanning (5-6 leaves per individual species sample), and then packed into 10 cm^3 plastic pots for magnetic measurements (at the Centre for Environmental Magnetism and Palaeomagnetism, Lancaster University).

2.3 Magnetic measurements

Measurements were made of anhysteretic remanent magnetization (ARM) and the saturation remanence (SIRM) of the leaves pre- and post-exposure (see Supporting Information). ARM is sensitive to the presence of ferrimagnetic particles with a mean particle size of ~25 nm[59]. The SIRM indicates the total concentration of magnetic particles on the preand post-exposure leaves. ARM was induced using a Molspin A. F. demagnetiser, with ARM attachment, generating a dc biasing field (0.08 mT) in the presence of an alternating field (100 milliTesla (mT) peak field). The ARM was measured using a spinner magnetometer (JR-6A, AGICO). The susceptibility of ARM (χ_{ARM}) was calculated by normalizing the ARM by the dc biasing field.

Room temperature remanent magnetization (IRM) was then incrementally acquired (in dc fields of 100 and 300 mT) using a Molspin pulse magnetizer. Calibration of the magnetometer was performed, on a regular basis, using a cross-calibrated rock sample (56.05×10^{-8} Am^2). All samples were measured in triplicate; the average value of each magnetic parameter was normalised for the leaf surface area (in m^2).

2.4 Metals analysis

The leaf-deposited PM was also evaluated by an acid wash procedure and analysis of metal concentrations using inductively coupled plasma-mass spectrometry (ICP-MS). Two leaves from each species, pre- and post-exposure, were washed thoroughly using purified 2% HNO_3 (the background metals concentration in 2% HNO_3 shown in Fig. S3) into acid-cleaned centrifuge tubes. The resultant, replicate leachates were then analysed for Mn, Fe, Co, Ni, Cu, Zn, Ti, V, Cr, As, Zr, Mo, Se, Cd, Sn, Sb, Pt and Pb using a Perkin Elmer quadrupole NexION 350D ICP-MS instrument. The metal concentrations reported here represent the average concentrations. The elements Se, Cd, Sn, Sb, Pt and Pb were measured under non-pressurised conditions (standard mode) whereas the remaining elements were measured in a collision cell with kinetic energy discrimination (collision mode) using helium gas. Metal compositions in the stock acid wash solution were well below 25 ng L^{-1}, except for Ti (< 65 ng L^{-1}) and Zn (< 201 ng L^{-1}), most likely a contribution from tubing used during the ICP-MS analysis.

2.5 Electron Microscopy

To identify UFP capture sites, leaves of the most effective species (silver birch) were examined using scanning electron microscopy (SEM) and energy dispersive spectroscopy (EDAX). Three leaf discs (10 mm diameter) of the pre- and post-exposure silver birch leaves were cut with a clean ceramic blade and coated with a thin layer (< 5 nm) of gold using an ion sputter. Each leaf disc was degassed (for 3 h at 0.7 bar), mounted on an aluminium stub over double-sided sticky tape and their microstructure examined with an SEM (FEI Quanta 650, FEI, Hillsboro, Oregon, USA) operating at an accelerating voltage of 10 or 20 kV. Elemental mapping was performed with an Oxford energy-dispersive X-ray spectrometer (EDAX). To reduce detection levels below the typical limit (~1000 ppm by weight), spectra were collected after acquisition times of up to 5 min. At least 5 spots from each leaf (before and after exposure) were analysed by EDAX.

2.6 *Statistical Analysis.*

Removal efficiencies were calculated using the following equation:

$$R_{eff(i)}(\%) = \frac{PNC_{upwind(i)} - PNC_{downwind(i)}}{PNC_{upwind(i)}} \times 100 \quad (1)$$

where R_{eff} (%) is the removal efficiency, PNC_{upwind} is the particle number concentration upwind in the wind tunnel experiment (#/cm^3), $PNC_{downwind}$ is the PNC downwind (#/cm^3), and i is the different particle size bins (i.e., 9.8-874.8 nm, 9.8-30 nm, 30-100 nm, 100-300 nm and 300-874.8 nm).

The Kolmogorov-Smirnov and Levene tests were used to verify the assumption of normality and the homogeneity of variances for the magnetic data (ARM, IRM_{100}, IRM_{300} and SIRM) and metal concentrations. One way analysis of variances (ANOVA) was carried out to investigate the effects of the plant species, and time intervals on the magnetic data. The significance of differences among the plant species were checked with Tukey's test (p = 0.05). The differences in metal concentrations among plant species were also tested by ANOVA and Tukey's test. Differences in metal concentrations between pre- and post-exposure leaves were tested using student's t test for each species. The data were analysed with SPSS software (ver. 20.0, IBM Corp, Armonk, NY).

3. Results and discussion

3.1 *UFP removal efficiency of different plant species*

The measured mean PNC for the diesel exhaust (in the absence of vegetation) was ~25×10^5/cm^3 (Fig. 1). There is no obvious increase in PNC upwind of the tested vegetation species compared with the no-vegetation case (Fig. S3, Supporting Information);

occasionally, the upwind PNCs are slightly lower, perhaps indicating some upward deflection of UFPs away from the central CPC measurement point.

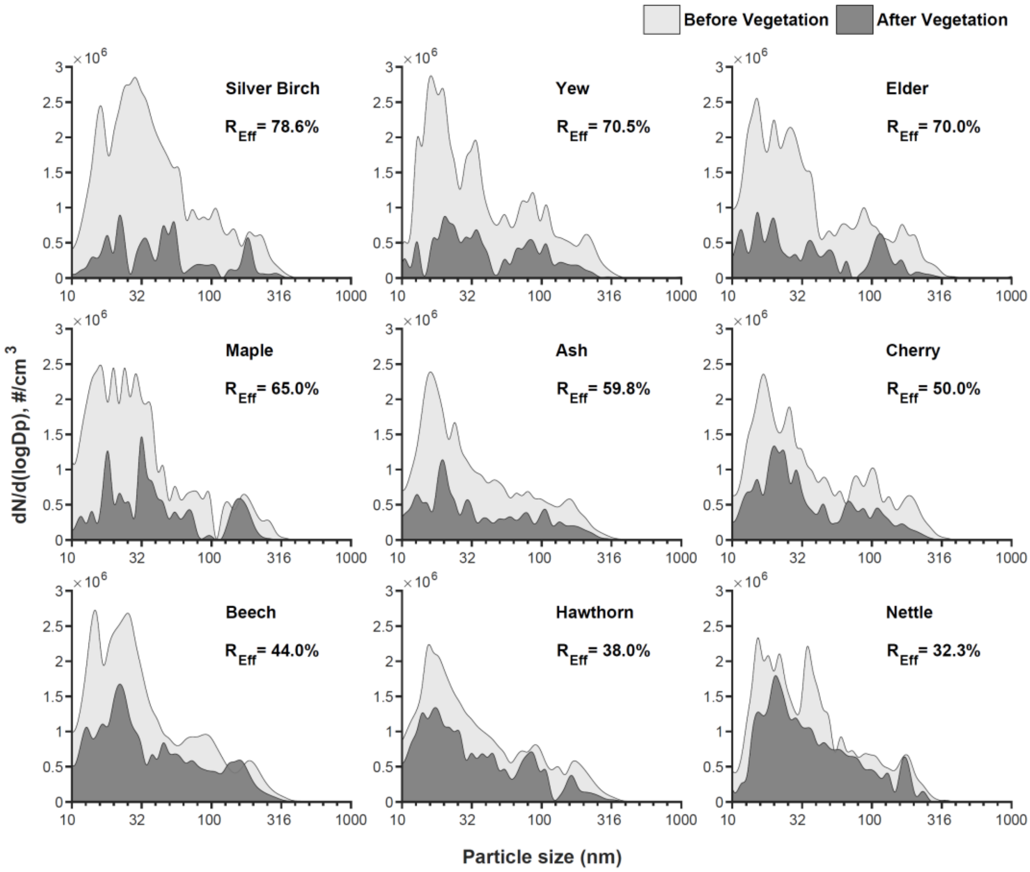

Fig. 1. Mean particle number distribution pre- and post-exposure (35 mins) of each vegetation species to the diesel exhaust (‘Before Vegetation’ = upwind of vegetation block; ‘After Vegetation’ = downwind of vegetation block). R_{Eff} (%) indicate the removal efficiency of UFPs by each species.

The average number size distributions of the UFPs, both in the absence of, and upwind and downwind from the vegetation displayed two major peaks, at 16 and 26 nm (nucleation mode), and a subsidiary peak of accumulation mode (soot) particles at ~100 nm (Figs. 1 and

S3). This distribution showed little change upwind and downwind for most of the plant species investigated, indicating the permeability of each tested vegetation block to the air stream. In marked contrast, measurements of $PM_{2.5}$ (by TSI, USA, SidePak AM520) upwind and downwind of a dense conifer species (juniper) identifies ‘blocking’ of air flow and resultant upwind enhancement of PNCs (Fig. S4). Some species induced slight increases in downwind mean particle size (see below).

Compared to the no-vegetation measurement, significant PNC reduction was measured downwind of most species tested, with much of the reduction occurring for the smaller particle sizes. Different plant species resulted in different removal efficiencies, reducing PNCs by up to ~79%. Silver birch is the most efficient species in removing UFPs, followed by yew>elder > maple > ash> cherry > beech > hawthorn > nettle (Fig. 1).

When the diesel exhaust had passed through the vegetation, the geomean diameter showed small but measurable increases, except in the case of hawthorn, elder and cherry (Table S3, Supporting Information). Silver birch and yew showed the largest mean increase in particle size, from 20.8 to 27.2 nm, and 19.3 to 29.6 nm, respectively, followed by maple (from 18.5 to 23.8 nm).

Dividing the PNC data into four size bins, 9.8−30 nm ($N_{9.8–30}$; nucleation mode), 30−100 nm ($N_{30–100}$; Aitken mode), 100−300 nm ($N_{100–300}$; accumulation mode) and 300−874.8 nm ($N_{9.8–30}$; coarse mode), the plants displayed differences in their removal of different particle size ranges (Fig. 2). For the nucleation mode (9.8−30 nm), silver birch removed the greatest particle numbers, followed by yew > elder > maple > cherry > ash > hawthorn > nettle. The nine different plant species followed this same order of removal efficiency for the PNCs in the accumulation and coarse modes.

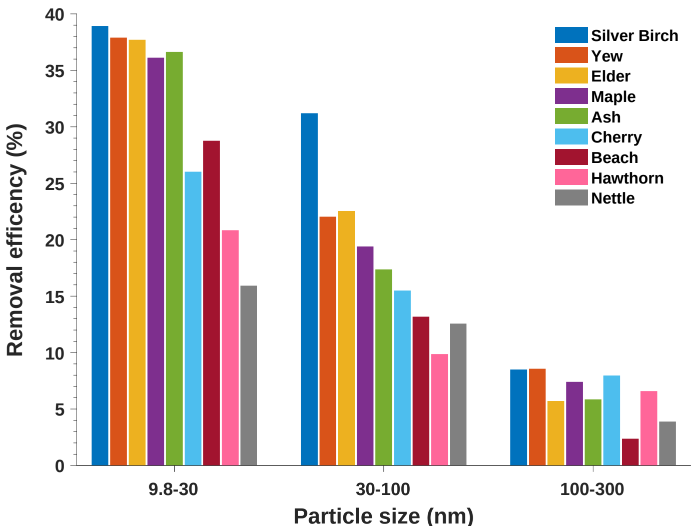

Fig. 2. The UFP removal efficiency of different plant species for different particle size bins.

3.2 Leaf magnetic values, magnetic mineralogy and grain sizes.

The pre- and post-exposure leaves display differences in ARM, IRM_{100}, IRM_{300} and IRM_{1000} (Fig. 3 A and B). The nettle and hawthorn displayed the highest pre-exposure magnetic content. For all but the hawthorn, the magnetic particle loadings on the leaves increased after their exposure to the diesel exhaust (Figs. 3 and S4 and 5; Fig. S3, Supporting Information). The ARM, IRM_{100}, IRM_{300} and SIRM of pre-exposure leaves ranged from ~5.0 to 22 $\times10^{-8}$A, 0.7 to 3 $\times10^{-6}$A, 1 to 4 $\times10^{-6}$A, and 1 to 4 $\times10^{-6}$A, respectively. The ARM, IRM_{100}, IRM_{300} and SIRM values of the exposed leaves ranged from ~13 to 35$\times10^{-8}$ A, 1 to 4.5 $\times10^{-6}$A, 2 to 6 $\times10^{-6}$A, and 2 to 6$\times10^{-6}$A, respectively.

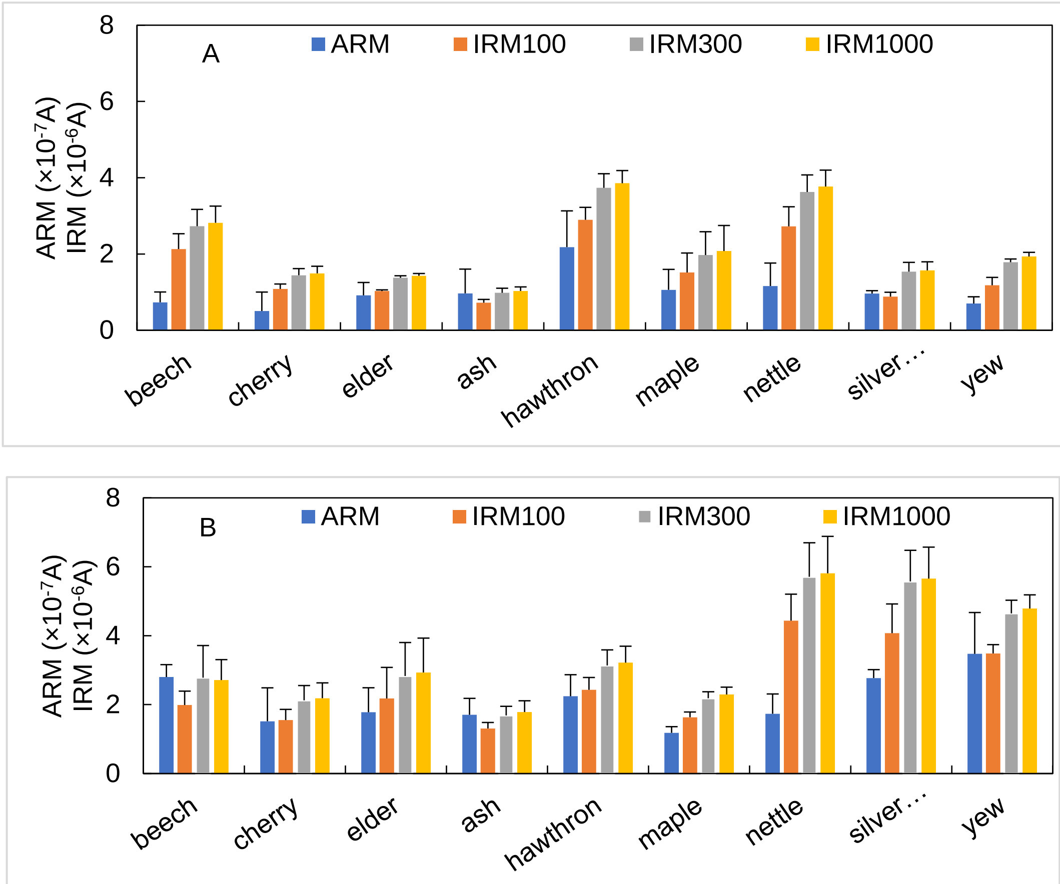

Figure 3. (A) Pre- and (B) post-exposure leaves display differences in magnetic particle loadings, as measured by ARM, IRM_{100}, IRM_{300} and IRM_{1000}

For each species, the leaf magnetic particle loadings, as measured by ARM, IRM_{100}, IRM_{300} and IRM_{1000}, vary through the successive periods of exhaust exposure. The silver birch leaves showed both the highest rate and most continuous accumulation of magnetic particles through the whole exposure period, followed by yew and elder, and then maple and nettle (Fig. S5, Supporting Information). Hawthorn showed little magnetic difference between pre-experiment and post-exposure leaves (Fig. S5B). Elder, maple, ash, cherry, beech and nettle all appear to reach a dynamic equilibrium (i.e. particle deposition balanced by particle re-suspension) in magnetic particle loadings within the timespan of the experimental exposure.

All leaves acquired most magnetic remanence at low applied fields; ~ 70% by 100 mT, and 95% by 300 mT (Table S2, Supporting Information). This indicates the presence of magnetically “soft” material (i.e., easily magnetized and demagnetized), such as magnetite (Fe_3O_4). Between 8% and 30% of the SIRM was acquired at higher applied fields (100 to 300 mT), indicating the presence of some maghemite and/or some nanoparticulate haematite[60]. The acquisition of some additional remanence (mostly ~1 to 2%, max 8%) at highest dc fields (> 300 mT) shows that magnetically ‘hard’ haematite also contributes to the leaf magnetic mineralogy. Given that haematite is much more weakly magnetic than magnetite, then up to ~40 times more haematite than magnetite may have deposited on the leaves during exposure to the diesel exhaust stream.

The different plant species also showed different leaf χ_{ARM}/SIRM values after exposure to the exhaust. Silver birch leaves had the highest χ_{ARM}/SIRM values, ranging from 62 to 138 $\times 10^{-5} A^{-1}$, with successive increases with exposure time. Because ARM is particularly sensitive to the presence of ultrafine magnetite particles, around 30 nm in size[59], χ_{ARM}/IRM_{300} values can be used as a rough estimate of magnetite grain size.

The magnetic particles present on the pre-exposure silver birch leaves were in the size range of ≤ 100 nm (Fig. S6, Supporting Information). After 20 minutes’ exposure to the diesel exhaust, the magnetic grain size of the particles deposited on the silver birch leaves decreased to ~ 20 nm in size. When the exposure time increased from 20 to 35 mins, the magnetic particle size increased to ~70 nm. In contrast, the size of the magnetic particles on nettle leaves was in the range of ~200 − 600 nm (Fig. S6, Supporting Information).

3.3 Metal concentrations of leaf-deposited PM

The concentrations of Mn, Fe, Cu and Zn on the post-exposure leaves were much higher than the other metals analyzed (Fig. 4). The metal contributions, post-exposure, are as follows: Mn > Zn > Fe > Cu > Ni > Ti > Cr > Pb > As > Se >Cd > V > Co > Zr > Mo > Pt. The very high Mn concentrations probably arise from the use of the diesel fuel additive, methylcyclopentadienyl manganese tricarbonyl (MMT) and/or from engine, especially cylinder, wear. The latter source, together with lubricating oil, is also likely to contribute the observed concentrations of Zn, Fe, Cu, and Cr[13]. The post-exposure metal concentrations from the leaf-deposited PM differed significantly between plant species (Fig. 4 and Table S4, Supporting Information). The highest metal concentrations were found in the leaf leachates from the silver birch, followed by yew and maple.

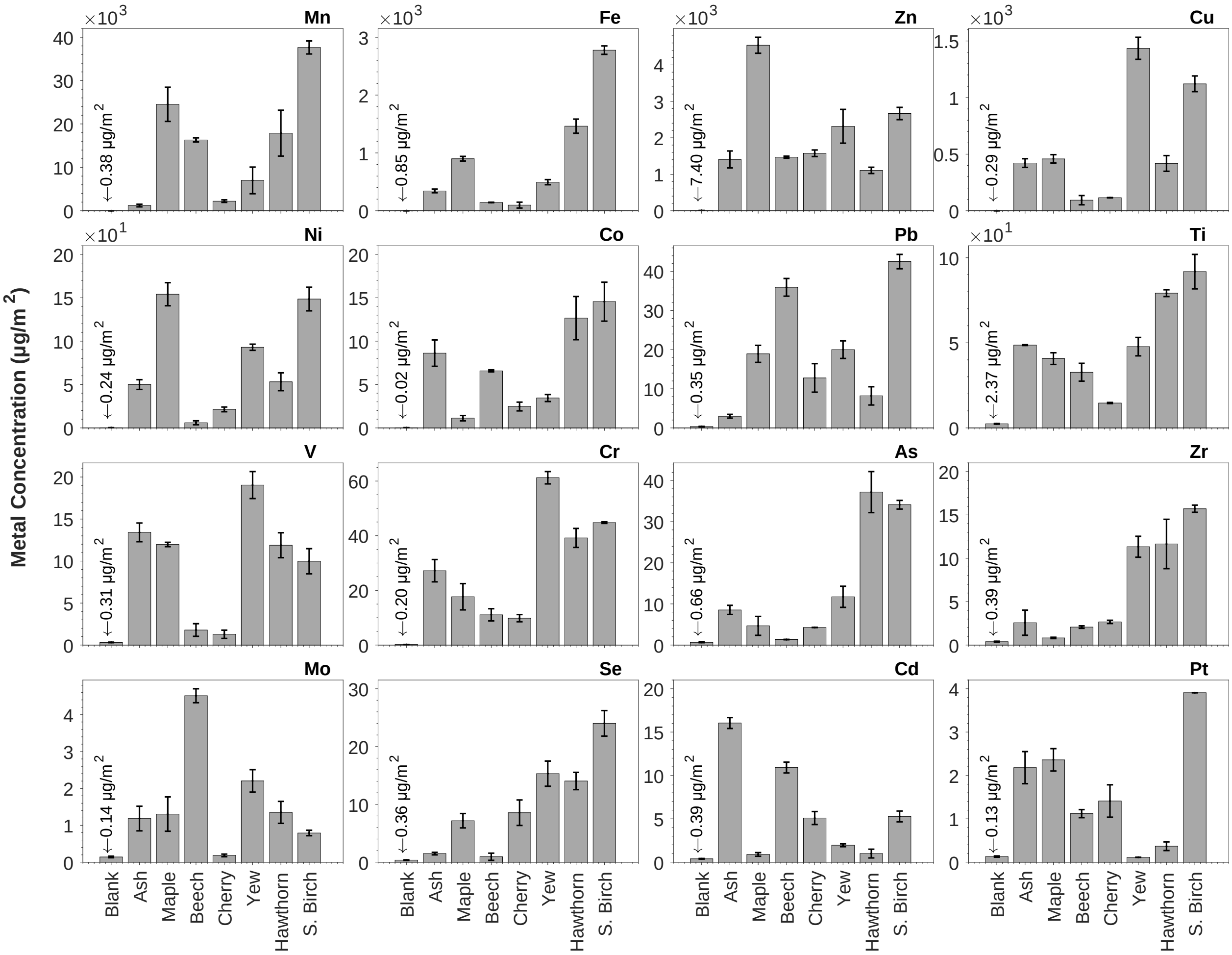

Fig. 4 Metal concentrations of leaf leachates post-exposure (i.e. metal concentrations$_{\text{post-exposure}}$ – metal concentrations$_{\text{pre-exposure}}$). ICP-MS data expressed as µg metal per m^2 of leaf surface area.

3.4 SEM-EDX

Scanning electron micrographs (Figs. 5 and 6) show the typical rough, hairy morphology of the adaxial leaf surfaces of the most efficient species, silver birch, which is hypostomatic

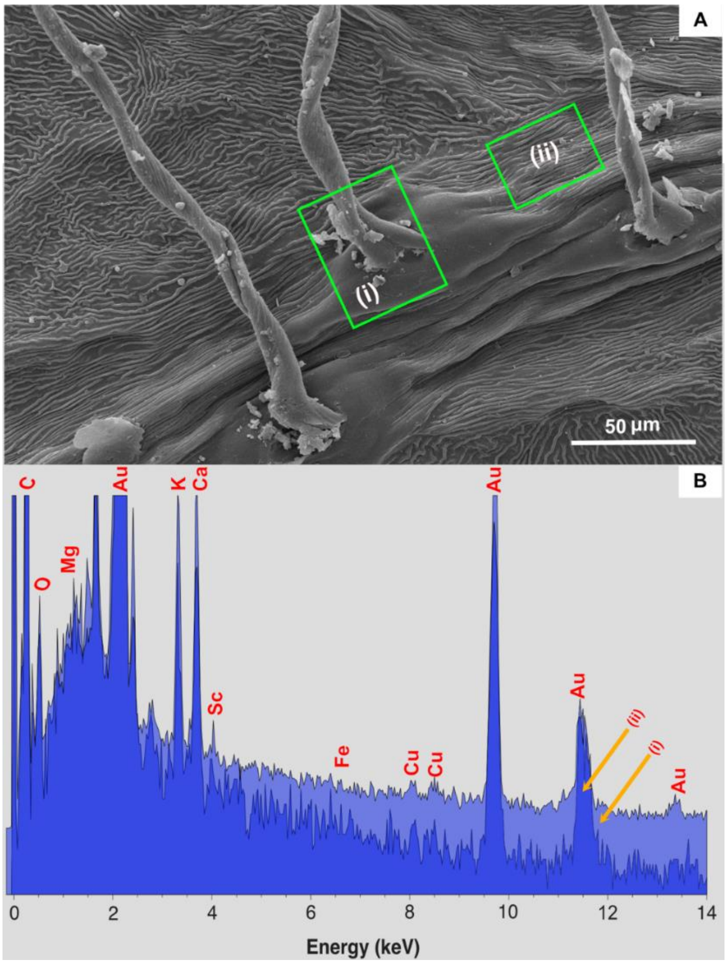

Fig. 5 (A) Scanning electron micrograph of the adaxial surface of the pre-exposure silver birch leaf, and (B) EDAX spectra for the leaf-deposited PM in sub-areas (i) and (ii) of image (A). (Note that the sample was gold-coated).

i.e., stomata occur only on the underside of the leaves. SEM-EDAX analysis of the silver birch leaf surfaces shows very low content of transition metal-bearing PM on the pre-exposure leaves

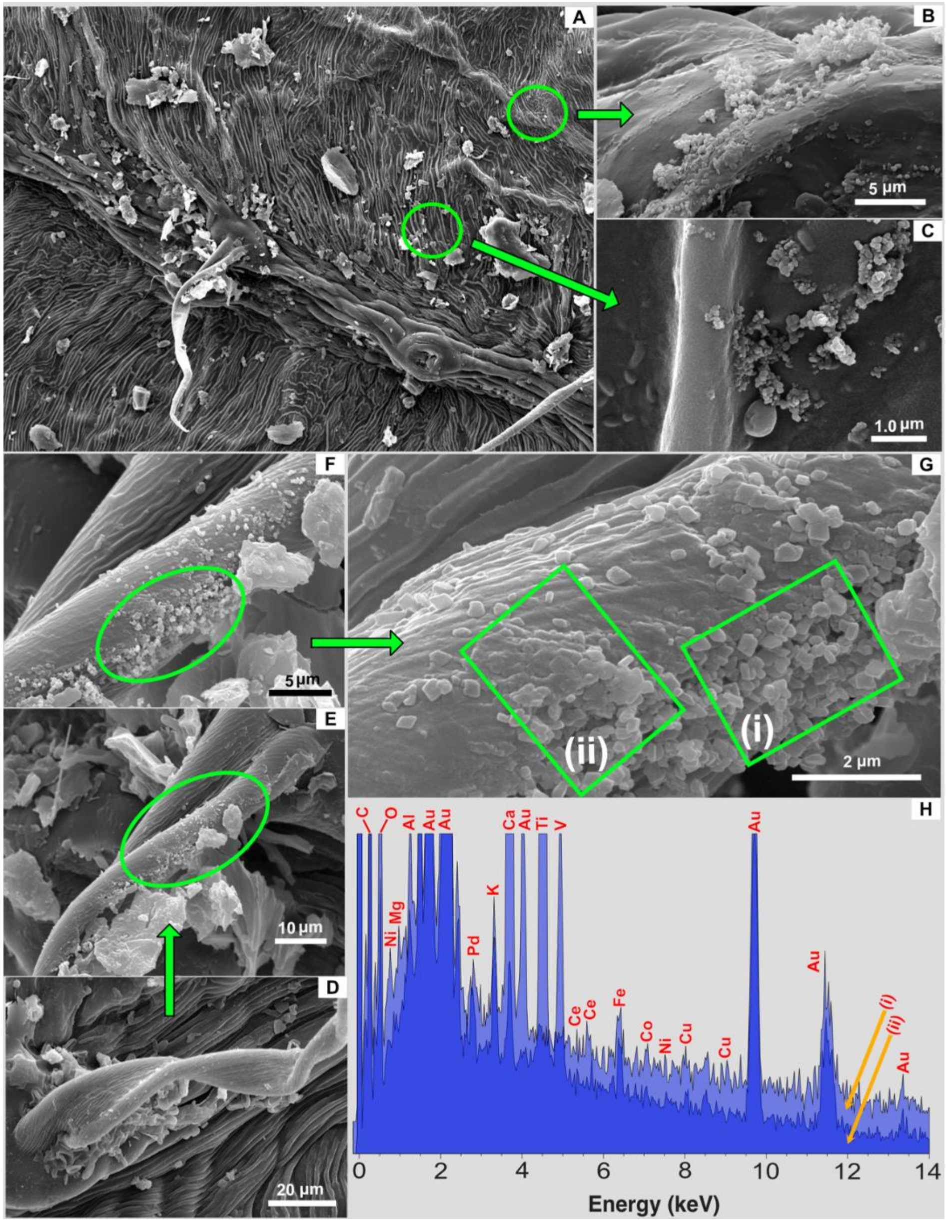

Fig. 6 (A) – (G): Scanning electron micrographs of the post-exposure silver birch leaves, and (H) EDAX spectra of the deposited particles shown in areas (i) and (ii) in micrograph (G).

(Fig. 5). In contrast, post-exposure, the silver birch surface displays an abundance of particles within the $PM_{2.5}$ range (Fig. 6), displaying a range of particle sizes and morphologies, including aggregated rounded chains of particles (Fig. 5C and Fig. S7), and discrete geometric particles (Fig. 6G). The post-exposure accumulation of UFPs within the micro-indentations of the rough leaf surface, and along and around the leaf hairs is noteworthy. These locations appear to be 'hot spots' for capturing UFPs; and may also act as gateways for UFP access to the leaf interior structure.

Prior to exposure, the major PM elemental contributions comprise C, O, Mg, K, and Ca (Fig. 5B). In contrast, the post-exposure birch leaves display higher concentrations of UFPs containing a much broader elemental range; specifically, the presence of Ni, Fe, Ti, V, Ce, Al, Pd, Cu and Co (Fig. 6H).

4. Discussion

These wind-tunnel experiments show that some plant species (silver birch, yew, elder, maple and ash) display UFP removal efficiencies as high as ~60 to 80%, demonstrating that selected plant species can act as effective UFP 'sinks' in the urban environment. Similar magnitudes of PM removal have been reported in real-world contexts for silver birch (for PM_1, Maher et al.[12]), and mixed woodland in Birmingham, U.K. (for PM estimated at 0.7 µm, Fowler et al.[52]).

Silver birch displayed both peak UFP removal values (~80%) and peak removal of particles < 30 nm. It continued to accumulate the finest magnetic particles (< ~20 nm) for 20 mins. of exposure, and then accumulated slightly larger and/or agglomerated PM (~70 nm) through to the end of the experiment. It is thus the most efficient of our sampled species in removing diesel exhaust UFPs; followed by yew and elder. Some of the sampled species (e.g.

ash, cherry) display magnetic evidence of both particle deposition and re-suspension through the time sequence of exposure.

Although nettle and hawthorn appear to be the least efficient plant species, their pre-exposure magnetic particle loading was higher than the other sampled species. This suggests they may have been 'pre-loaded' with airborne PM, and effectively at or close to a dynamic equilibrium between the rates of particle deposition and loss by re-suspension. In the real world, leaves can continue to accumulate particles (rather than attain equilibrium with ambient PM concentrations) through rainfall wash-off[39] and entry of PM into the leaf structure via stomata and/or wax cuticle overgrowth[61].

Leaf surface characteristics and size appear critical regarding PM deposition. Particles are more readily deposited on smaller leaves, with shorter petioles, surface roughness, especially in the form of leaf trichomes, and/or mucilage[12, 36, 38-39, 62-64]. Phoretic effects, in response to gradients in turbulence[65]), chemical and/or electric potential[66], may enhance UFP deposition along leaf hairs.

Here, we also found that when the diesel exhaust passed through some of the sampled species, the geomean diameter increased downwind of the vegetation, showing that these plants (silver birch, yew, maple) removed more of the smallest UFPs, possibly of greatest potential hazard to human health.

For our most efficient species, silver birch, many of the UFPs deposited on the post-exposure leaves were rich in transition metals, including Mn, Ni, Fe, Al, Cr, V, Ti and Cu, together with the anti-knock and catalytic converter metals, Ce and Pd. Most of the magnetic remanence-capable particles deposited on the post-exposure silver birch leaves were < 100 nm. Nanoparticles of this size can penetrate the body very efficiently[2], even bypassing the blood-brain barrier via the olfactory bulb[4-5]. Similarly, Maher et al.[5, 12] found that many particles deposited on the leaves of silver birches installed at a busy roadside (Lancaster, U.K.) were < 200 nm, exhibited spherical or semi-spherical morphologies, and were Fe-rich. Such Fe-rich particles, abundant and typical of condensation droplets released from high-temperature combustion and frictional (brakewear) processes, are likely to contribute much of the measured magnetic remanence of the plant leaves. Particles rich in transition metals might cause oxidative stress by direct generation of reactive oxygen species not only in lung and cardiovascular cells but also in the brain[5]. Oxidative brain damage is a characteristic of most types of neurodegenerative disease, including Alzheimer's and Parkinson's disease.

All of the data reported here are consistent with the efficient interception and capture of vehicle-derived UFPs by plant leaves, rather than airflow impedance or perturbation, or physical screening effects and "fumigation" of the upwind zone. (In marked contrast, similar experiments on juniper indicate 'blocking' of airflow, and resultant enhancement of upwind PNCs).

Given the health impacts of exposure to traffic-derived PM, it is essential to understand, and optimise, the mitigation potential of roadside vegetation, in order to guide policy appropriately. In the UK, for instance, even reducing the annual average concentration of $PM_{2.5}$ by only 1 $\mu g/m^3$ would result in a saving of ~3.6 million life years, equivalent to an increase in life expectancy of 20 days in people born in 2008[67]. It is thus timely to improve and update the available data and information regarding PM removal rates by leaf deposition, in order to optimise selection and design of new roadside planting.

Under-estimation by most CFD modelling studies of the potential for substantial PM removal by designed vegetation has negative impacts on policy and potential mitigation. Adoption of realistic, species-specific particle deposition velocities (i.e. up to ~50 times higher than the values of 0.1, 0.2 and 0.64 cm s^{-1} commonly employed for $PM_{2.5}$) and an appropriate, microscale approach, at road user-relevant heights[35], are both essential.

In summary, these data indicate that selected plant species can remove by surface deposition substantial amounts (> 50%) of ultrafine exhaust-derived PM, and of the heavy metals contained within the high particle number concentrations of this PM fraction. Fast, non-destructive magnetic measurements provide an effective indicator of leaf particle deposition. Scanning electron microscopy can identify the major micro-sites associated with greatest particle accumulation. Hence, roadside planting of carefully-selected and managed plant species can effectively mitigate exposure of road users and adjacent residents (especially vulnerable groups like school children) to UFP pollution near major roads. Careful testing and selection of the most efficient species can readily improve air quality.

Acknowledgements

We are grateful for financial support from Natural Science Basic Research Plan in Shaanxi Province of China (2017JQ4014) and the Research Program of Ministry of Housing and Urban-Rural Development of the People's Republic of China (2018-K2-006). We also are grateful to

Andy Baker, Engineering Department, Lancaster University for assistance with the wind tunnel and the diesel vehicle.

Supporting Information Available: 26 pages, 7 figures and 4 tables. This material is available free of charge via the Internet at http://pubs.acs.org.

References

1. Liu, J. Y.; Hsiao, T. C.; Lee, K. Y.; Chuang, H. C.; Cheng, T. J.; Chuang, K. J. Association of ultrafine particles with cardiopulmonary health among adult subjects in the urban areas of northern Taiwan. *Sci. Total Environ.* **2018**, *627*: 211-215.
2. Miller, M. R.; Raftis, J. B.; Langrish, J. P.; McLean, S. G.; Samutrtai, P.; Connell, S. P.; Wilson, S.; Vesey, A. T.; Fokkens, P. H. B.; Boere, A. J. F.; Krystek, P.; Cambell, C. J.; Hadoke, W. F.; Donaldson, K.; Cassee, F. R.; Newby, D. E.; Duffin, R.; Mills, N. L. Inhaled nanoparticles accumulate at sites of vascular disease. *ACS nano.* **2017**, *11*(5): 4542-4552.
3. Stone, V.; Miller, M. R.; Clift, M. J. D.; Elder, A.; Mills, N. L.; Møller, P.; Schins, R. P. F.; Vogel, U.; Kreyling, W. G.; Jensen, K. A.; Kuhlbusch, T. A. J.; Schwarze, P. E.; Hoet, P.; Pietroiusti, A.; Vizcaya-Ruiz, A. D.; Baeza-Squiban, A.; Teixeira, J. P.; Tran, C. L.; Cassee, F. R. Nanomaterials versus ambient ultrafine particles: an opportunity to

exchange toxicology knowledge. *Environ. Health Perspect.* **2017**, *125*(10): 106002. DOI: 10.1289/EHP424

4. Oberdörster, G.; Sharp, Z.; Atudorei, V.; Elder, A.; Gelein, R.; Kreyling, W.; Cox, C. Translocation of inhaled ultrafine particles to the brain. *Inhal. Toxicol.* **2004**, *16*(6-7): 437-445.
5. Maher, B. A.; Ahmed, I. A. M.; Karloukovski, V.; MacLaren, D. A.; Foulds, P. G.; Allsop, D.; Mann, D. M. A.; Torres-Jardón, R.; Calderon-Garduenas, L. Magnetite pollution nanoparticles in the human brain. *P Natl. Acad. Sci. USA.* **2016**, *113*(39): 10797-10801.
6. Bakand, S.; Hayes, A.; Dechsakulthorn, F. Nanoparticles: a review of particle toxicology following inhalation exposure. *Inhal. Toxicol.* **2012**, *24*(2): 125-135.
7. Donaldson, K.; Stone, V.; Seaton, A.; MacNee, W. Ambient particle inhalation and the cardiovascular system: potential mechanisms. *Environ. Health Perspect.* **2001**, *109*(4): 523-527.
8. Karlsson, H. L.; Gustafsson, J.; Cronholm, P.; Möller, L. Size-dependent toxicity of metal oxide particles—a comparison between nano-and micrometer size. *Toxicol. Lett.* **2009**, *188*(2): 112-118.
9. Rückerl, R.; Schneider, A.; Breitner, S.; Cyrys, J.; Peters, A. Health effects of particulate air pollution: a review of epidemiological evidence. *Inhal. Toxicol.* **2011**, *23*(10): 555-592.
10. Hama, S. M. L.; Cordell R L.; Monks, P. S. Quantifying primary and secondary source contributions to ultrafine particles in the UK urban background. *Atmos. Environ*. **2017**,

166: 62-78.

11. Shi, J. P.; Harrison, R. M.; Brear, F. Particle size distribution from a modern heavy duty diesel engine. *Sci. Total Environ.* **1999**, *235*(1-3): 305-317.
12. Maher, B. A.; Ahmed, I. A. M.; Davison, B.; Karloukovski, V.; Clarke, R. Impact of roadside tree lines on indoor concentrations of traffic derived particulate matter. *Environ. Sci. Technol.* **2013**, *47*: 13737-13744.
13. Liati, A.; Schreiber, D.; Dimopoulos Eggenschwiler, P.; Arroyo Rojas Dasilva, Y. Metal particle emissions in the exhaust stream of diesel engines: an electron microscope study. *Environ. Sci. Technol.* **2013**, *47*(24): 14495-14501.
14. Zhu, Y. F.; Hinds, W. C.; Kin, S.; Sioutas, C. Concentration and size distribution of ultrafine particles near a major highway. *Air Waste Manage. Assoc.* **2002**, *52*: 1032-1042.
15. Liati, A.; Pandurangi, S. S.; Boulouchos, K.; Schreiber, D.; Arroyo Rojas Dasilva, Y. Metal nanoparticles in diesel exhaust derived by in-cylinder melting of detached engine fragments. *Atmos. Environ*. **2015**, *101*: 34-40.
16. Kukutschová, J.; Moravec, P.; Tomášek, V.; Matějka, V.; Smolík, J.; Schwarz, J.; Seiderová, J.; Šafářová, K.; Filip, P. On airborne nano/micro-sized wear particles released from low-metallic automotive brakes. *Environ. Pollut.* **2011**, *159*(4): 998-1006.
17. Mathissen, M.; Scheer, V.; Vogt, R.; Benter, T. Investigation on the potential generation of ultrafine partilces from the tire-road interface. *Atmos. Environ*. **2011**, *45*(34): 6172-6179.
18. Yang, Y.; Vance, M.; Tou, F. Y.; Tiwari, A.; Liu, M.; Hochella Jr, M. F. Nanoparticles in road dust from impervious urban surfaces: distribution, identification, and environmental

implications. *Environ. Sci. Nano.* **2016**, *3*(3): 534-544.

19. Verma, V.; Shafer, M. M.; Schauer, J. J.; Sioutas, C. Contribution of transition metals in the reactive oxygen species activity of PM emissions from retrofitted heavy-duty vehicles. *Atmos. Environ*. **2010**, *44,* 5165-5173.

20. Sanderson, P.; Su, S. S.; Chang, I. T. H.; Delgado Saborit, J. M.; Kepaptsoglou, D. M.; Weber, R. J. M.; Harrison, R. M. Characterisation of iron-rich atmospheric submicrometre particles in the roadside environment. *Atmos. Environ*. **2016**, *140*: 167-175.

21. Harrison, R. M.; Shi, J. P.; Xi, S. H.; Khan, A.; Mark, D.; Kinnersley, R.; Yin, J. X. Measurement of number, mass and size distribution of particles in the atmosphere. *Philos. T. Roy. Soc. A.* **2000**, *358*(1775): 2567-2580.

22. Heal, M. R.; Kumar, P.; Harrison, R. M. Particles, air quality, policy and health. *Chem. Soc. Rev.* **2012**, *41*(19): 6606-6630.

23. Robert, M. A.; Kleeman, M. J.; Jakober, C. A. Size and composition distributions of particulate matter emissions: Part 2—Heavy-duty diesel vehicles. *J. Air Waste Manage. Assoc.* **2007**, *57*(12): 1429-1438.

24. Robert, M. A.; VanBergen, S.; Kleeman, M. J.; Jakober, C. A. Size and composition distributions of particulate matter emissions: Part 1—Light-duty gasoline vehicles. *J. Air Waste Manage. Assoc.* **2007**, *57*(12): 1414-1428.

25. Jayaratne, E. R.; He, C.; Ristovski, Z. D.; Morawska, L.; Johnson, G. R. A comparative investigation of ultrafine particle number and mass emissions from a fleet of road-road diesel and CNG buses. *Environ. Sci. Technol.* **2008**, *42*: 6736-6742.

26. Herner, J. D.; Hu, S. H.; Robertson, W. H.; Huai, T.; Chang, M. C. O.; Rieger, P.; Ayala, A. Effect of advanced aftertreatment for PM and NOx reduction on heavy-duty diesel engine ultrafine particle emissions. *Environ. Sci. Technol.* **2011**, *45*(6): 2413-2419.

27. Su, D. S.; Serafino, A.; Müller, J. O.; Jentoft, R. E.; Schlögl, R.; Fiorito, S. Cytotoxicity and inflammatory potential of soot particles of low-emission diesel engines. *Environ. Sci. Technol.* **2008**, *42*(5): 1761-1765.

28. Air Quality Expert Group. Impacts of vegetation on urban air pollution. **2018**, 1-40. https://uk-https://uk-air.defra.gov.uk/assets/documents/reports/cat09/1807251306 180509_Effects_of_vegetation_on_urban_air_pollution_v12_final.pdf

29. Janhäll, S. Review on urban vegetation and particle air pollution–Deposition and dispersion. *Atmos. Environ*. **2015**, *105*: 130-137.

30. Jeanjean, A. P. R.; Monks, P. S.; Leigh, R. J. Modelling the effectiveness of urban trees and grass on $PM_{2.5}$ reduction via dispersion and deposition at a city scale. *Atmos. Environ*. **2016**, *147*: 1-10.

31. Jeanjean, A. P. R.; Buccolieri, R.; Eddy, J.; Monks, P. S.; Leigh, R. J. Air quality affected by trees in real street canyons: The case of Marylebone neighbourhood in central London. *Urban For. Urban Green.* **2017**, *22*: 41-53.

32. Nowak, D. J.; Hirabayashi, S.; Bodine, A.; Hoehn, R. Modeled $PM_{2.5}$ removal by trees in ten US cities and associated health effects. *Environ. Pollut.* **2013**, *178*: 395-402.

33. Vos, P. E. J.; Maiheu, B.; Vankerkom, J.; Janssen, S. Improving local air quality in cities: to tree or not to tree? *Environ. Pollut.* **2013**, *183*: 113-122.

34. Abhijith, K. V.; Kumar, P.; Gallagher, J.; MaNabola, A.; Baldauf, R.; Pilla, F.; Broderick, B.; Di Sabatino, S.; Pulvirenti, B. Air pollution abatement performances of green infrastructure in open road and built-up street canyon environments–A review. *Atmos. Environ*. **2017**, *162*: 71-86.

35. Santiago, J. L.; Martilli, A.; Martin, F. On dry deposition modelling of atmospheric pollutants on vegetation at the microscale: Application to the impact of street vegetation on air quality. *Bound.-Layer Meteor.* **2017**, *162*(3): 451-474.

36. Burkhardt, J.; Peters, K.; Crossley, A. The presence of structural surface waxes on coniferous needles affects the pattern of dry deposition of fine particles. *J. Exp. Bot.* **1995**, *46*(7): 823-831.

37. Beckett, K. P.; Freer-Smith, P. H.; Taylor, G. Particulate pollution capture by urban trees: effect of species and windspeed. *Glob. Change Biol.* **2000**, *6*(8): 995-1003.

38. Thönnessen, M. Elementdynamik in fassadenbegrünendemWilden Wein (*Parthenocissus tricuspidata*). Nährelemente, Anorganische Schadstoffe, Platin-Gruppen-Elemente, Filterleistung, Immissionshistorische Aspekte, Methodische Neu-undWeiterentwicklungen. – Kölner Geographische Arbeiten, Heft 78, Geographisches Institut, Universität Köln 2002; pp 103.

39. Mitchell, R.; Maher, B. A.; Kinnersley, R. Rates of particulate matter pollution deposition onto leaf surfaces: temporal and inter-species magnetic analyses. *Environ. Pollut.* **2010**, *158*: 1472-1478.

40. Weber, F.; Kowarik, I.; Säumel, I. Herbaceous plants as filters: Immobilization of

particulates along urban street corridors. *Environ. Pollut.* **2014**, *186*: 234-240.

41. *Airborne particulate matter in the United Kingdom*; Third report to the Department of the Environment; Quality of Urban Air Review Group (QUARG); HMSO, London, 1996; http://worldcat.org/isbn/0952077132.

42. Gallagher, M. W.; Beswick, K. M.; Duyzer, J.; Westrate, H.; Choularton, T. W.; Hummelshøj, P. Measurements of aerosol fluxes to Speulder forest using a micrometeorological technique. *Atmos. Environ*. **1997**, *31*(3): 359-373.

43. Freer-Smith, P. H.; Beckett, K. P.; Taylor, G. Deposition velocities to *Sorbus aria*, *Acer campestre*, *Populus deltoides* × *trichocarpa* 'Beaupré', *Pinus nigra* and × *Cupressocyparis leylandii* for coarse, fine and ultra-fine particles in the urban environment. *Environ. Pollut.* **2005**, *133*(1): 157-167.

44. Pugh, T. A. M.; Mackenzie, A. R.; Whyatt, J. D.; Hewitt, C. N. Effectiveness of green infrastructure for improvement of air quality in urban street canyons. *Environ. Sci. Technol.* **2012**, *46*(14): 7692-7699.

45. Nowak, D. J.; Crane, D. E.; Stevens, J. C. Air pollution removal by urban trees and shrubs in the United States. *Urban For. Urban Green.* **2006**, *4*(3): 115-123.

46. Litschke, T.; Kuttler, W. On the reduction of urban particle concentration by vegetation–a review. *Meteorol. Z.* **2008**, *17*(3): 229-240.

47. Jin, S. J.; Guo, J. K.; Wheeler, S.; Kan, L. Y.; Che, S. Q. Evaluation of impacts of trees on $PM_{2.5}$ dispersion in urban streets. *Atmos. Environ*. **2014**, *99*: 277-287.

48. Bonn, B.; von Schneidemesser, E.; Butler, T.; Churkina, G.; Ehlers, C.; Grote, R.; Klemp,

D.; Nothard, R.; Schäfer, K.; von Stülpnagel, A.; Kerschbaumer, A.; Yousefpour, R.; Fountoukis, C.; Lawrence, M. G. Impact of vegetative emissions on urban ozone and biogenic secondary organic aerosol: Box model study for Berlin, Germany. *J. Clean Prod.* **2018**, *176*: 827-841.

49. Calfapietra, C.; Fares, S.; Manes, F.; Morani, A.; Sgrigna, G.; Loreto, F. Role of Biogenic Volatile Organic Compounds (BVOC) emitted by urban trees on ozone concentration in cities: A review. *Environ. Pollut.* **2013**, *183*: 71-80.

50. Hoffmann, T.; Odum, J. R.; Bowman, F.; Atmospheric, D. C. J. O. Formation of organic aerosols from the oxidation of biogenic hydrocarbons. *J. Atmos. Chem.* **1997**, *26*, 189-222.

51. Matzka, J.; Maher, B. A. Magnetic biomonitoring of roadside tree leaves: identification of spatial and temporal variations in vehicle-derived particulates. *Atmos. Environ*. **1999**, *31*: 4565-4569.

52. Fowler, D.; Skiba, U.; Nemitz, E.; Choubedar, F.; Branford, D.; Donovan, R.; Rowland, P. Measuring aerosol and heavy metal deposition on urban woodland and grass using inventories of ^{210}Pb and metal concentrations in soil. *Water Air Soil Pollut. Focus.* **2004**, *4*: 483-499.

53. Baldauf, R.; Thoma, E.; Khlystov, A.; Isakov, V.; Bowker, G.; Long, T.; Snow, R. Impacts of noise barriers on near-road air quality. *Atmos. Environ*. **2008**, *42*(32): 7502-7507.

54. Al-Dabbous, A. N.; Kumar, P. The influence of roadside vegetation barriers on airborne nanoparticles and pedestrians exposure under varying wind conditions. *Atmos. Environ*. **2014**, *90*(90): 113-124.

55. Lin, M. Y.; Hagler, G.; Baldauf, R.; Isakov, V.; Lin, H. Y.; Khlystov, A. The effects of vegetation barriers on near-road ultrafine particle number and carbon monoxide concentrations. *Sci. Total Environ.* **2016**, *553*: 372-379.

56. Lin, M. Y.; Khlystov, A. Investigation of ultrafine particle deposition to vegetation branches in a wind tunnel. *Aerosol Sci. Technol.* **2011**, *46*: 465-472.

57. Hwang, H. J.; Yook, S. J.; Ahn, K. H. Experimental investigation of submicron and ultrafine soot particle removal by tree leaves. *Atmos. Environ*. **2011**, *45*: 6987-6994.

58. Davison, B.; Whyatt, D.; Boardman, C. Aerosol evolution from a busy road in North-west England. *Meteorogische Zeitschrift*. **2008**, *18*(1): 55-60.

59. Maher, B. A. Magnetic properties of some synthetic sub-micro magnetites. *Geophys. J. Int.* **1988**, *94*: 83-96.

60. Maher, B. A.; Karloukovski, V. V.; Mutch, T. J. High-field remanence properties of synthetic and natural submicrometre haematites and goethites: significance for environmental contexts. *Earth Planet. Sci. Lett.* **2004**, *226*(3-4): 491-505.

61. Lehndorff, E.; Urbat, M.; Schwark, L. Accumulation histories of magnetic particles on pine needles as function of air quality. *Atmos. Environ*. **2006**, *40*(36): 7082-7096.

62. Wang, H. X.; Shi, H.; Li, Y. Y.; Zhang, J. Seasonal variations in leaf capturing of particulate matter, surface wettability and micromorphology in urban tree species. *Front. Env. Sci. Eng.* **2013**, *7*(4): 579-588.

63. Liu, J. Q.; Cao, Z. G.; Zou, S. Y.; Liu, H. H.; Hai, X.; Wang, S. H.; Duan, J.; Xi, B. Y.; Yan, G. X.; Zhang, S. W.; Jia, Z. K. An investigation of the leaf retention capacity,

efficiency and mechanism for atmospheric particulate matter of five greening tree species in Beijing, China. *Sci. Total Environ.* **2018**, *616-617*: 417-426.

64. Weerakkody, U.; Dover, J. W.; Mitchell, P.; Reiling, K. Evaluating the impact of individual leaf traits on atmospheric particulate matter accumulation using natural and synthetic leaves. *Urban For. Urban Green.* **2018**, *30*: 98-107.

65. Hicks, B. B.; Saylor, R. D.; Baker, B. D. Dry deposition of particles to canopies—A look back and the road forward. *J. Geophys. Res.-Atmos.* **2016**, *121*(24): 14691-14707.

66. Moran, J. L.; Posner, J. D. Phoretic self-propulsion. *Annu. Rev. Fluid Mech.* **2017**, *49*: 511-540.

67. *The mortality effects of long-term exposure to particulate air pollution in the United Kingdom*; Committee on the Medical Effects of Air Pollutants, Department of Health, London, UK, 2010; http://comeap.org.uk/documents/reports/128-the-mortality-effects-of-long-term-exposure-toparticulate-air-pollution-in-the-uk.html.

TOC

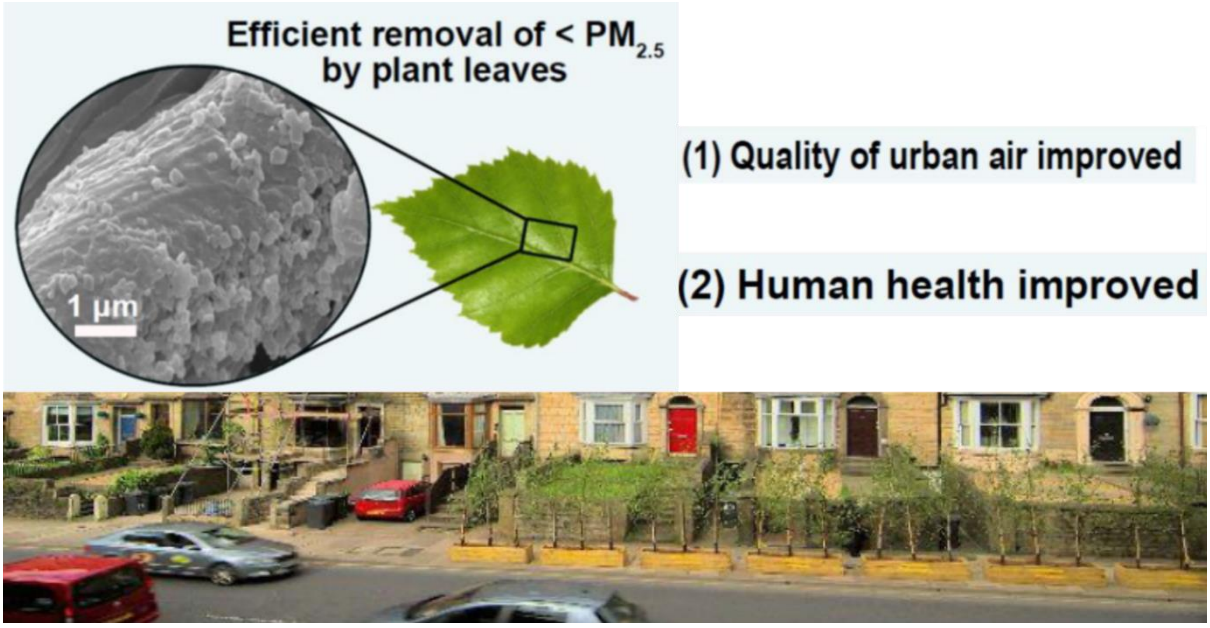
Efficient removal of < $PM_{2.5}$
by plant leaves
1 µm
(1) Quality of urban air improved
(2) Human health improved